

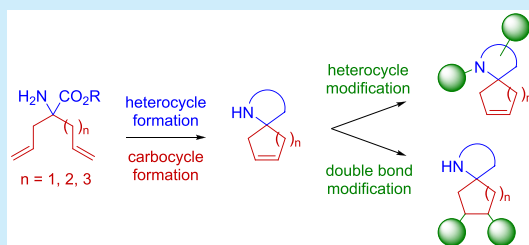
Spirocycles as Rigidified sp^3 -Rich Scaffolds for a Fragment Collection

Attila Sveicz, Andrew J. P. North, Natalia Mateu,* Sarah L. Kidd, Hannah F. Sore, and David R. Spring*

Department of Chemistry, University of Cambridge, Lensfield Road, Cambridge, CB2 1EW, U.K.

Supporting Information

ABSTRACT: Novel divergent methodology to access sp^3 -rich spirocyclic fragments is reported. First, a robust modular synthesis of bis-alkene amino ester building blocks was developed. Three different carbocycles and six heterocycles were then constructed to assemble eight spirocycles. Importantly, strategic exit vectors were incorporated within each scaffold to aid fragment growth and were elaborated via chemical modifications. Finally, computational methods demonstrate higher levels of rigidity, three-dimensionality, and structural diversity of the library compared to a commercial collection.



Since the rise of fragment-based drug discovery (FBDD) over two decades ago this strategy has proven particularly effective, producing numerous clinical candidates and two FDA-approved drugs, Vemurafenib¹ and Venetoclax² (Figure 1A). The success of this approach can be linked to two main benefits. First, due to the considerably fewer number of possible fragment-sized molecules, the chemical space coverage of a relatively small fragment library is exceedingly more efficient than that of a vast high-throughput screening (HTS) library. Second, fragment hits possess fewer but nonetheless high-quality binding interactions with the protein target, which

can be later elaborated to afford highly potent lead compounds.^{3–7}

Within this paradigm the generation of a suitable screening library is paramount. However, despite the undoubted success of FBDD, within recent years organic synthesis has been identified as a significant bottleneck within this process, owing to the overrepresentation of predominantly “flat” (hetero)-aromatic fragments lacking three-dimensionality as well as synthetically tractable exit vectors that could be utilized in rapid structure–activity relationship (SAR) studies.^{4,5,8} While complexity of fragments remains under debate within the literature,^{9,10} importantly, more three-dimensional (3D) fragments displaying exit vectors increase the potential for multidirectional fragment growth and the ability to identify leads for challenging targets such as protein–protein interactions.^{8,11} Thus, recent efforts from within the synthetic community have focused on the development of novel strategies to access 3D fragments.^{12–15}

Spirocyclic motifs remain an important bioactive substructure appearing within several natural products^{16–18} and FDA-approved drugs^{19,20} (Figure 1B). Importantly, as a direct result of their architecture, these small molecules often provide several advantages.²¹ First, the spiranic center generates an inherently 3D structure that gives rise to higher levels of complexity, a feature which has been linked to improved clinical success.^{10,22,23} Moreover, the conformationally restricted nature of spirocycles can reduce both the conformational entropy penalty of target binding and the number of possible conformations (distinct 3D shapes) that a molecule can adopt leading to higher potency and selectivity, respectively.^{24,25} However, despite their utility, these motifs remain underrepresented in fragment screening collections. Indeed, very few compounds within the ChemBridge spirocycle library meet the size criteria of FBDD,^{26,27} while only

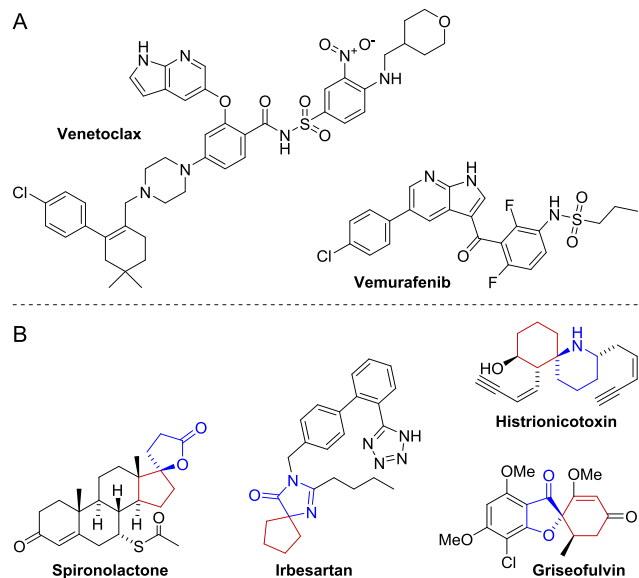


Figure 1. (A) Two FBDD-derived FDA-approved drugs: Venetoclax and Vemurafenib. (B) Examples of spirocyclic natural products (Griseofulvin and Histrionicotoxin) and FDA-approved drugs (Spirolactone and Irbesartan).

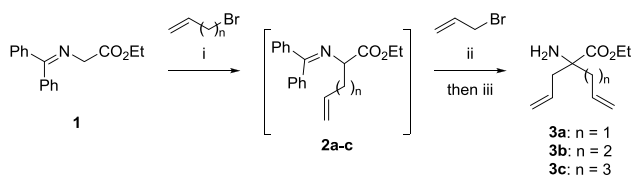
Received: April 29, 2019

three spirocycles feature within the Maybridge core fragment collection. Thus, there is an urgent need for spirocyclic fragments and calls from within the field have encouraged the development of novel strategies to access such motifs.²⁵

While strategies to access spirocycles within sp^3 -rich screening libraries have been reported, they either do not solely seek to construct spirocycles^{28–30} or focus on more complex bis-³¹ and bridged-³² spirocycles. In addition, these compounds often lie outside the requirements for FBDD. Thus, we envisaged that a novel approach to access diverse spirocyclic fragments containing a polar heterocycle and a lipophilic carbocycle could give rise to a valuable library complementing already existing screening collections. To achieve this, our efforts were directed at utilizing α,α -disubstituted amino acid derivatives as building blocks, providing the potential to exploit the functional handles to generate fragment-like spirocyclic scaffolds. The incorporation of the two alkene handles enabled the carbocycle formation via ring-closing metathesis (RCM), forming an essential alkene exit vector, allowing us to alter the properties of this portion of the fragments. In addition, the amino and ester functionalities were installed to enable diverse heterocycle formations, increasing the possible polar interactions and the overall water solubility of the fragments. Accordingly, rapid access to varied scaffolds and the potential to exploit the exit vectors for fragment growth and merging to aid hit-to-lead development was envisioned.

First, the building blocks were prepared through the double alkylation of the glycine Schiff base **1** to form building blocks **3a–c** (Scheme 1). Despite similar procedures having been

Scheme 1. Synthesis of the Building Blocks



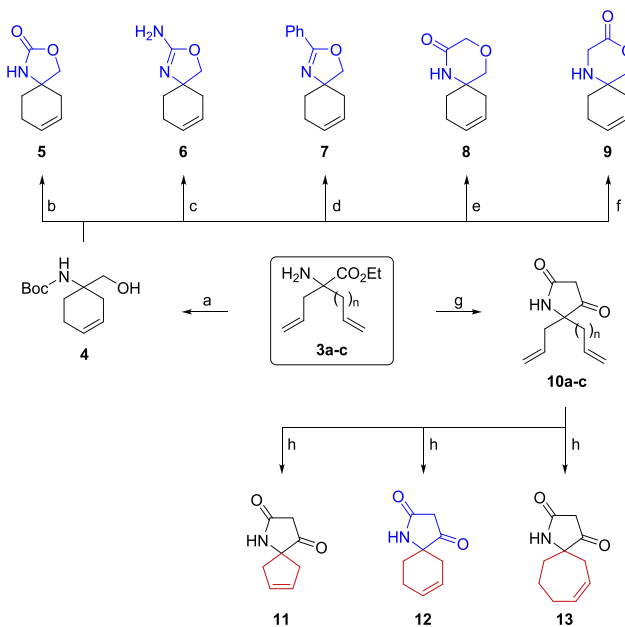
^aReaction conditions: (i) $t\text{BuOK}$, THF; (ii) $t\text{BuOK}$, THF; (iii) HCl, THF/ H_2O ; then Na_2CO_3 . Overall yields **3a**: 67% (steps i and ii the same, steps i–iii in one pot); **3b**: 61% (steps i–iii in one pot); **3c**: 31% (steps i–iii done stepwise).

reported before,^{33–36} herein we describe the straightforward racemic synthesis of α -quaternary amino esters with two different alkyl chains bearing terminal alkenes (**3b,c**). A brief optimization of the related literature procedure³³ allowed us to form **3c** in a simple stepwise process. Further optimization of the analogous route, however, resulted in the development of a one-pot procedure removing the chromatographic steps to access **3b** on large-scale in an improved 61% yield. This approach also enabled the formation of **3a**.

Subsequently, investigations into the formation of the different heterocycles were pursued using the racemic amino ester building block **3b**. First, the amine was Boc-protected to allow the cyclohexene formation in an RCM, followed by the reduction of the ester to the hydroxymethyl group by LiBH_4 to afford the key intermediate **4** in good yield. Intramolecular base-mediated pairing between the alcohol and Boc groups could then be achieved forming the oxazolidone moiety in **5**. The removal of the Boc protecting group under acidic conditions could be followed by pairing reactions incorporat-

ing various reagents. Reaction with cyanogen bromide formed amino oxazoline **6** whereas ethyl benzimidate hydrochloride gave the phenyl-substituted oxazoline **7**. The two morpholinones **8** and **9** were constructed by the chemoselective alkylation/acylation with chloroacetyl chloride and phenyl bromoacetate respectively (Scheme 2).

Scheme 2. Synthesis of Different Core Heterocycles and Carbocycles^a

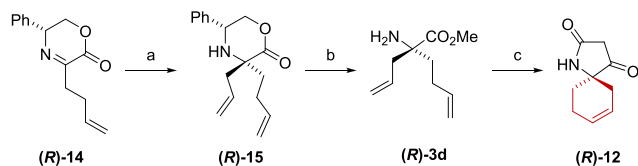


^aReaction conditions: (a) (i) Boc_2O , THF, 85%; (ii) Grubbs II, CH_2Cl_2 , 81%; (iii) LiBH_4 , THF, 89%; (b) $t\text{BuOK}$, THF, 90%; (c) HCl, dioxane; then BrCN , Et_3N , EtOH , 58%; (d) HCl, dioxane; then ethyl benzimidate hydrochloride, Et_3N , DCE, 57%; (e) (i) HCl, dioxane; then chloroacetyl chloride, Et_3N , CH_2Cl_2 , 57%; (ii) $t\text{BuOK}$, $t\text{BuOH}$, 99%; (f) HCl, dioxane; then phenyl bromoacetate, $i\text{Pr}_2\text{NEt}$, MeCN , 43%; (g) (i) ethyl malonyl chloride, Et_3N , CH_2Cl_2 , 73–81%; (ii) $t\text{BuOK}$, THF; then aq. HCl, THF, 86–92%; (h) Grubbs II, CH_2Cl_2 , 69–99%.

Building block **3b** could also be acylated with ethyl malonyl chloride, and then the base-mediated cyclization onto the ester group followed by the acid-catalyzed decarboxylative hydrolysis yielded the tetramic acid intermediate **10b**. Formation of the carbocycle ring in an RCM gave **12** in a good yield. To exemplify the potential to expand the cyclohexene ring, spirocycles also featuring the five- and seven-membered carbocycles were also synthesized from **3a** and **3c**, respectively (Scheme 2). Importantly, all the spirocycles were synthesized in no more than five steps from the building blocks.

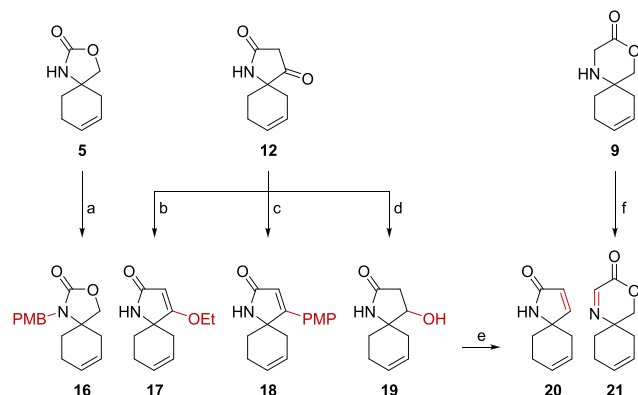
Although racemic compounds were sought for our fragment library, the ability to produce optically pure isomers e.g. for SAR studies was also crucial. Thus, a second asymmetric route to the desired building blocks was devised utilizing the well-precedented stereoselective alkylation of iminolactones derived from phenylglycinol.^{37,38} In this case, only one diastereomer of the aminolactone (*R*)-**15** was observed, which was successively deprotected to form the optically pure building block (*R*)-**3d**. As proof of concept, the single *R*-enantiomer of **12**, with the spiro[4,5] scaffold, was also synthesized (Scheme 3).

With eight fragment scaffolds in hand, it was next crucial to demonstrate the utility of the exit vectors installed within the

Scheme 3. Enantioselective Synthesis of (R)-12^a

^aReaction conditions: (a) allyl bromide, Zn, DMF, 68%; (b) (i) SOCl₂, MeOH; (ii) Pb(OAc)₄, MeOH/CH₂Cl₂; then HCl, H₂O, 92% over 2 steps; (c) (i) ethyl malonyl chloride, Et₃N, CH₂Cl₂, 46%; (ii) *t*BuOK, THF; then aq. HCl, THF, 92%; (iii) Grubbs II, CH₂Cl₂, 97%.

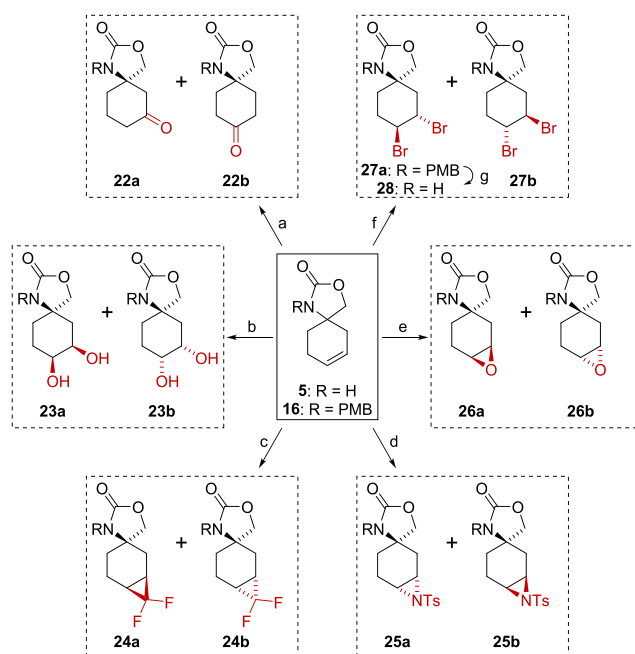
molecules. Thus, *N*-alkylation of the oxazolidone (16), *O*-alkylation (17), and cross-coupling of the tetramic acid (18) were demonstrated. In addition, a modified heterocycle with an alcohol functionality (19) and two with new double bonds (20 and 21) were synthesized, incorporating new exit vectors to the resultant molecules (Scheme 4).

Scheme 4. Heterocycle Modification^a

^aReaction conditions: (a) PMBCl, NaH, DMF, 96%; (b) KHMDS, EtBr, THF, 54%; (c) (i) Tf₂O, Et₃N, CH₂Cl₂, 59%; (ii) PMPB(OH)₂, Pd(PPh₃)₄, Na₂CO₃, H₂O/THF, 73%; (d) NaBH₄, MeOH, 23%; (e) TFAA, Et₃N, CH₂Cl₂; then KHCO₃, MeOH, 30%; (f) Pb(OAc)₄, MeCN, 92%.

Finally, to exhibit the versatility of the double bond as an exit vector, modifications such as Wacker oxidation (22a,b), dihydroxylation (23a,b), difluoro-cyclopropanation (24a,b), aziridination (25a,b), epoxidation (26a,b), and dibromination (27a,b) were explored (Scheme 5). Initial attempts of the epoxidation of 5, however, proved challenging with respect to the isolation and purification of 26a,b. Thus, a PMB group was installed (16) indeed proving to be compatible with several reaction conditions generating the diversified fragments in good to excellent yields. Removal of the PMB protecting group was also exemplified by the treatment of compound 27a with CAN to generate the unprotected modified spirocycle 28.

The physicochemical properties of our library consisting of 28 different nonprotected spirocyclic molecules were then calculated and compared to the commercially available Maybridge core fragment library using the widely accepted guidelines from within the field (Table 1).^{26,27} This revealed the spirocyclic library adheres well to the guidelines and was additionally predicted to be significantly less lipophilic (SlogP of 0.9 versus 1.8) and more rigid (rotatable bond count of 0.2 versus 2.0) than the Maybridge core fragment collection.

Scheme 5. Double Bond Modification and PMB Deprotection^a

^aR = PMB unless specified otherwise. All products are racemic. Reaction conditions (combined yields with ratios a/b are given): (a) Fe(acac)₃, *t*BuOH, air, 47%, 1.9:1; (b) OsO₄, NMO, citric acid, H₂O/THF, 99%, 2.5:1; (c) TMSCF₃, NaI, THF, 62%, 20:1; (d) TsNClNa·3H₂O, PhNMe₃Br₃, 4 Å MS, 70%, 1.4:1; (e) R = H, mCPBA, NaHCO₃, CH₂Cl₂, 52%, 8:1; (f) PhNMe₃Br₃, CH₂Cl₂, 96%, 18:1; (g) CAN, MeCN/H₂O, 96% (R = H in product).

Table 1. Physicochemical Properties of Fragment Libraries Compared to the Ideal Range

property ^a	spirocycles ^b	Maybridge ^c	ideal range ^d
MW	186 ± 41	182 ± 42	140–230
HBD	1.3 ± 0.7	1.0 ± 0.8	≤3
HBA	1.8 ± 0.6	1.9 ± 0.7	≤3
SlogP	0.9 ± 0.9	1.8 ± 0.8	0–2
RBC	0.2 ± 0.5	2.0 ± 1.5	≤3
TPSA	48 ± 13	39 ± 14	≤60

^aMW = molecular weight (Da), HBD = number of hydrogen-bond donors, HBA = number of hydrogen-bond acceptors, SlogP = partition coefficient, RBC = rotatable bond count, TPSA = topological polar surface area (Å²). ^bProtecting groups virtually removed from our library. ^cMaybridge core fragment collection of 1000 fragments. ^dGuidelines set by Astex Pharmaceuticals.^{26,27} See Supporting Information.

Strikingly, our library also displayed far superior sp³-content with an average fraction of sp³ atoms (Fsp³) of 0.52, which also translates into a much lower fraction of aromatic atoms (Faro) of 0.16. Moreover, the average number of chiral centers (1.6) is also considerably higher, resulting in greater stereochemical diversity achieved by the spirocyclic fragments.

In order to qualitatively assess the shape diversity in our library, a principal moments of inertia (PMI) analysis was carried out. Our library was then compared to the whole Maybridge core fragment collection of 1000 fragments and a

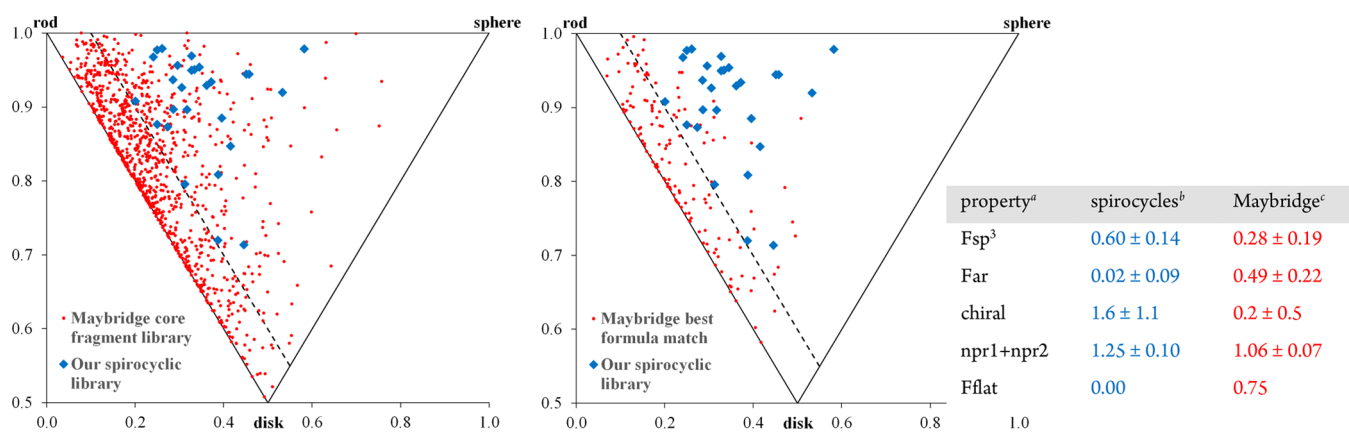


Figure 2. PMI plots for the visual representation of shape diversity. Each corner of the plot represents a unique shape (rod-, disk-, and sphere-like features). The dashed line represents the boundary of “flat land”.¹¹ Our virtual deprotected library of 28 spirocycles (blue) is compared to 1000 fragments (red, left) and the 147 best-matched fragments based on heavy and heteroatom count (red, right) from the Maybridge collection. The table on the right summarizes the physicochemical properties used to describe the 3D properties of the two libraries. ^aFsp³ = fraction of sp³ atoms, Far = fraction of aromatic atoms, chiral = number of chiral centers, npr = normalized PMI ratio, Fflat = fraction of molecules lying below the “flat land line”.¹¹ ^bVirtual deprotected library. ^c147 best-matched fragments from the Maybridge collection. See [Supporting Information](#).

representative subset consisting of the 147 best-matched compounds based on heavy atoms (Figure 2). Both plots show that the Maybridge fragments tend to aggregate to the left-hand edge (rod- and disc-like features) or the “flat land”, whereas our spirocyclic fragments are more evenly distributed. Analysis showed that more than 70% of the whole Maybridge collection and 75% of the best formula match subset fall within “flat land” (defined as $npr1 + npr2 \leq 1.1$).¹¹ On the other hand, no spirocyclic fragment in our library was found below the “flat land” criteria, suggesting more 3D molecules.

In conclusion, we have developed a robust, scalable, and modular route to racemic α,α -disubstituted amino ester building blocks including an adapted stereoselective alkylation protocol to access the optically pure intermediate. These were utilized in the efficient construction of eight novel spirocyclic scaffolds comprising pharmacophore heterocycles and variable carbocycles. All core scaffolds display an array of 3D exit vectors demonstrated by a number of chemical modifications to both the hetero- and carbocycles. Together with the enantioselective synthesis, rapid SAR studies and binding pocket exploration by fragment growth could therefore be envisioned. Finally, the computational predictions revealed optimal physicochemical properties, higher rigidity increased 3D properties, shape, and stereochemical diversity compared to a commercial fragment library.

■ ASSOCIATED CONTENT

● Supporting Information

The Supporting Information is available free of charge on the [ACS Publications website](#) at DOI: [10.1021/acs.orglett.9b01499](https://doi.org/10.1021/acs.orglett.9b01499).

General Remarks, Procedures and Analytical Data, Computational Analysis, Crystallographic Data, and NMR Spectra (PDF)

Accession Codes

CCDC [1912266–1912268](#) and [1912283–1912289](#) contain the supplementary crystallographic data for this paper. These data can be obtained free of charge via www.ccdc.cam.ac.uk/data_request/cif, or by emailing data_request@ccdc.cam.ac.uk, or by contacting The Cambridge Crystallographic Data

Centre, 12 Union Road, Cambridge CB2 1EZ, UK; fax: +44 1223 336033.

■ AUTHOR INFORMATION

Corresponding Authors

*E-mail: spring@ch.cam.ac.uk.

*E-mail: nm462@ch.cam.ac.uk.

ORCID

David R. Spring: [0000-0001-7355-2824](https://orcid.org/0000-0001-7355-2824)

Notes

The authors declare no competing financial interest.

■ ACKNOWLEDGMENTS

A.S. acknowledges support from the Walters family and Selwyn College, University of Cambridge. A.J.P.N., H.F.S., and D.R.S. acknowledge support from the Engineering and Physical Sciences Research Council (EP/P020291/1). N.M.S. thanks the EU for a Marie Curie Fellowship (2013-IEF-626191). S.L.K. thanks AstraZeneca for funding. D.R.S. acknowledges support from the Royal Society (Wolfson Research Merit Award). The Spring lab acknowledges general lab support from the ERC, EPSRC, BBSRC, MRC, and Royal Society. The authors would like to thank Dr. Andrew Bond (Department of Chemistry, University of Cambridge) for carrying out the single-crystal crystallography for the project.

■ REFERENCES

- (1) Bollag, G.; Hirth, P.; Tsai, J.; Zhang, J.; Ibrahim, P. N.; Cho, H.; Spevak, W.; Zhang, C.; Zhang, Y.; Habets, G.; et al. *Nature* **2010**, *467*, 596–599.
- (2) Souers, A. J.; Levenson, J. D.; Boghaert, E. R.; Ackler, S. L.; Catron, N. D.; Chen, J.; Dayton, B. D.; Ding, H.; Sampath, D.; Lee, J.; et al. *Nat. Med.* **2013**, *19*, 202–208.
- (3) Scott, D. E.; Coyne, A. G.; Hudson, S. A.; Abell, C. *Biochemistry* **2012**, *51*, 4990–5003.
- (4) Boyd, S. M.; Turnbull, A. P.; Walse, B. *Comput. Mol. Sci.* **2012**, *2*, 868–885.
- (5) Keserü, G. M.; Erlanson, D. A.; Ferenczy, G. G.; Hann, M. M.; Murray, C. W.; Pickett, S. D. *J. Med. Chem.* **2016**, *59*, 8189–8206.
- (6) Murray, C. W.; Rees, D. C. *Nat. Chem.* **2009**, *1*, 187–192.

- (7) Hajduk, P. J.; Greer, J. *Nat. Rev. Drug Discovery* **2007**, *6*, 211–219.
- (8) Murray, C. W.; Rees, D. C. *Angew. Chem., Int. Ed.* **2016**, *55*, 488–492.
- (9) Hann, M. M.; Leach, A. R.; Harper, G. J. *Chem. Inf. Comput. Sci.* **2001**, *41*, 856–864.
- (10) Lovering, F. *MedChemComm* **2013**, *4*, 515–519.
- (11) Morley, A. D.; Pugliese, A.; Birchall, K.; Bower, J.; Brennan, P.; Brown, N.; Chapman, T.; Drysdale, M.; Gilbert, I. H.; Hoelder, S.; et al. *Drug Discovery Today* **2013**, *18*, 1221–1227.
- (12) Twigg, D. G.; Kondo, N.; Mitchell, S. L.; Galloway, W. R. J. D.; Sore, H. F.; Madin, A.; Spring, D. R. *Angew. Chem., Int. Ed.* **2016**, *55*, 12479–12483.
- (13) Mateu, N.; Kidd, S. L.; Kalash, L.; Sore, H. F.; Madin, A.; Bender, A.; Spring, D. R. *Chem. - Eur. J.* **2018**, *24*, 13681–13687.
- (14) Foley, D. J.; Doveston, R. G.; Churcher, I.; Nelson, A.; Marsden, S. P. *Chem. Commun.* **2015**, *51*, 11174–11177.
- (15) Hassan, H.; Marsden, S. P.; Nelson, A. *Bioorg. Med. Chem.* **2018**, *26*, 3030–3033.
- (16) Müller, G.; Berkenbosch, T.; Benningshof, J. C. J.; Stumpfe, D.; Bajorath, J. *Chem. - Eur. J.* **2017**, *23*, 703–710.
- (17) Oxford, A. E.; Raistrick, H.; Simonart, P. *Biochem. J.* **1939**, *33*, 240–248.
- (18) Kim, S.; Ko, H.; Lee, T.; Kim, D. *J. Org. Chem.* **2005**, *70*, 5756–5759.
- (19) Taylor, F. F.; Faloon, W. W. *J. Clin. Endocrinol. Metab.* **1959**, *19*, 1683–1687.
- (20) Brunner, H. R. *Am. J. Hypertens.* **1997**, *10*, 311S–317S.
- (21) Carreira, E. M.; Fessard, T. C. *Chem. Rev.* **2014**, *114*, 8257–8322.
- (22) Lovering, F.; Bikker, J.; Humblet, C. *J. Med. Chem.* **2009**, *52*, 6752–6756.
- (23) Zheng, Y.; Tice, C. M.; Singh, S. B. *Bioorg. Med. Chem. Lett.* **2014**, *24*, 3673–3682.
- (24) Wermuth, C. G.; Villoutreix, B.; Grisoni, S.; Olivier, A.; Rocher, J.-P. In *The Practice of Medicinal Chemistry*; Wermuth, C., Aldous, D., Raboisson, P., Rognan, D., Eds.; Academic Press: London, 2015; pp 73–96.
- (25) Zheng, Y.-J.; Tice, C. M. *Expert Opin. Drug Discovery* **2016**, *11*, 831–834.
- (26) Congreve, M.; Carr, R.; Murray, C.; Jhoti, H. *Drug Discovery Today* **2003**, *8*, 876–877.
- (27) Palmer, N.; Peakman, T. M.; Norton, D.; Rees, D. C. *Org. Biomol. Chem.* **2016**, *14*, 1599–1610.
- (28) Hung, A. W.; Ramek, A.; Wang, Y.; Kaya, T.; Wilson, J. A.; Clemons, P. A.; Young, D. W. *Proc. Natl. Acad. Sci. U. S. A.* **2011**, *108*, 6799–6804.
- (29) Mayol-Llinàs, J.; Farnaby, W.; Nelson, A. *Chem. Commun.* **2017**, *53*, 12345–12348.
- (30) Haftchenary, S.; Nelson, S. D.; Furst, L.; Dandapani, S.; Ferrara, S. J.; Bošković, Ž. V.; Lazú, S. F.; Guerrero, A. M.; Serrano, J. C.; Crews, D. K.; et al. *ACS Comb. Sci.* **2016**, *18*, 569–574.
- (31) Stotani, S.; Lorenz, C.; Winkler, M.; Medda, F.; Picazo, E.; Martinez, R. O.; Karawajczyk, A.; Sanchez-Quesada, J.; Giordanetto, F. *ACS Comb. Sci.* **2016**, *18*, 330–336.
- (32) Foley, D. J.; Craven, P. G. E.; Collins, P. M.; Doveston, R. G.; Aimon, A.; Talon, R.; Churcher, I.; von Delft, F.; Marsden, S. P.; Nelson, A. *Chem. - Eur. J.* **2017**, *23*, 15227–15232.
- (33) López, A.; Moreno-Mañas, M.; Pleixats, R.; Roglans, A.; Ezquerro, J.; Pedregal, C. *Tetrahedron* **1996**, *52*, 8365–8386.
- (34) Hammer, K.; Undheim, K. *Tetrahedron* **1997**, *53*, 2309–2322.
- (35) Kotha, S.; Sreenivasachary, N. *Bioorg. Med. Chem. Lett.* **1998**, *8*, 257–260.
- (36) Khan, I. U.; Kattela, S.; Hassan, A.; Correia, C. R. D. *Org. Biomol. Chem.* **2016**, *14*, 9476–9480.
- (37) Harwood, L. M.; Vines, K. J.; Drew, M. G. B. *Synlett* **1996**, *1996*, 1051–1053.
- (38) Fustero, S.; Mateu, N.; Albert, L.; Aceña, J. L. *J. Org. Chem.* **2009**, *74*, 4429–4433.